

# $\nu\bar{\nu}$ -Pair Synchrotron Emission in Neutron-Star Matter based on a Relativistic Quantum Approach

Tomoyuki Maruyama<sup>a,b</sup>, A. Baha Balantekin<sup>c,b</sup>, Myung-Ki Cheoun<sup>f,b</sup>, Toshitaka Kajino<sup>e,b,d</sup>, Grant J. Mathews<sup>g,b</sup>

<sup>a</sup>*College of Bioresource Sciences, Nihon University, Fujisawa 252-8510, Japan*

<sup>b</sup>*National Astronomical Observatory of Japan, 2-21-1 Osawa, Mitaka, Tokyo 181-8588, Japan*

<sup>c</sup>*Department of Physics, University of Wisconsin, Madison, WI 53706, USA*

<sup>d</sup>*Graduate School of Science, The University of Tokyo, Hongo 7-3-1, Bunkyo-ku, Tokyo 113-0033, Japan*

<sup>e</sup>*Beihang University, School of Physics, International Research Center for Big-Bang Cosmology and Element Genesis, Beijing 100083, China*

<sup>f</sup>*Department of Physics, Soongsil University, Seoul, 156-743, Korea*

<sup>g</sup>*Center of Astrophysics, Department of Physics, University of Notre Dame, Notre Dame, IN 46556, USA*

---

## Abstract

We study the  $\nu\bar{\nu}$ -pair synchrotron emission from electrons and protons in a relativistic quantum approach. This process occurs only in a presence of a strong magnetic field, and it is considered to be one of effective processes for neutron star cooling. In this work we calculate the luminosity of the  $\nu\bar{\nu}$ -pairs emitted from neutron-star-matter with a magnetic field of about  $10^{15}$  G. We find that the energy loss is much larger than that of the modified Urca process. The  $\nu\bar{\nu}$ -pair emission processes in strong magnetic fields is expected to contribute significantly to the cooling of the magnetars.

**Keywords:** Neutron-Star, Neutrino Emission, Strong Magnetic Field, Relativistic Quantum Approach

---

Magnetic fields in neutron stars play important roles in the interpretation of many observed phenomena. Magnetars, which are associated with super strong magnetic fields, [1, 2] have properties different from normal neutron stars. Thus, phenomena related magnetars can provide a lot of information about the physics of the magnetic field.

Magnetars emit energetic photons and are observed as soft gamma repeaters (SGR) and anomalous X-ray pulsars (AXPs) [3]. Furthermore, the surface temperature of magnetars is  $T \approx 0.28 - 0.72$  keV, which is larger than that of normal neutron stars  $T \approx 0.01 - 0.15$  keV at a similar age [7]. Thus, the associated strong magnetic fields may play a significant role in magnetars.

Many authors have paid attention into cooling processes of neutron stars (NS) because it gives important information on neutron star structure [5]. Neutron stars are cooled by neutrino emission, and a magnetic field is expected to affect the emission mechanism largely because a strong magnetic field can supply energy and momentum into the process.

Neutrino antineutrino ( $\nu\bar{\nu}$ )-pair emission is also an important cooling processes in the surface region of NSs. Pairs can be emitted by synchrotron radiation in a strong magnetic field [6, 7, 8, 9] and by bremsstrahlung through two particle collisions [10, 11].

The  $\nu\bar{\nu}$ -pair synchrotron radiation is allowed via  $p(e^-) \rightarrow p(e^-) + \nu + \bar{\nu}$  only in strong magnetic fields. Landstreet [6] studied this process for  $B \sim 10^{14}$  G and applied it to the cooling of white dwarfs.

In that study the magnetic field is very low, and the discontinuity due to the Landau levels was ignored when calculating the  $\nu\bar{\nu}$ -pair luminosity. It was concluded that this process is insignificant

van Dalen et al. [9] calculated the  $\nu\bar{\nu}$ -pair emission in a strong magnetic field of  $B \geq 10^{16}$  G. In such strong magnetic fields and low temperatures,  $T \leq 1$  MeV, energy intervals between two states with different Landau numbers are much larger than the temperature. Hence, they treated only the spin-flip transition between states with the same Landau number.

In Ref. [12, 13], we introduced Landau levels in our framework and calculated pion production through proton synchrotron radiation strong magnetic fields. In that work we showed that quantum calculations gave much larger production rates than semi-classical calculations.

In Ref. [14] we calculated the axion production in the same way, and found that the transition between two states with different Landau numbers gives significant contributions even if the temperature is low,  $T \leq 1$  keV, when the strength of the magnetic field is large,  $B = 10^{15}$  G. In this case the energy interval between the two states is much larger than the temperature.

In the present paper, then, we apply our quantum theoretical approach to  $\nu\bar{\nu}$ -pair synchrotron production in strong magnetic fields and calculate this through the transition between different Landau levels for electrons and protons. Only this quantum approach can exactly describe the momentum transfer from the magnetic field.

We assume a uniform magnetic field along the  $z$ -direction,  $\mathbf{B} = (0, 0, B)$ , and take the electromagnetic vector potential  $A^\mu$  to be  $A = (0, 0, xB, 0)$  at the position  $\mathbf{r} \equiv (x, y, z)$ .

The relativistic wave function  $\psi$  is obtained from the following Dirac equation:

$$\left[ \gamma_\mu \cdot (i\partial^\mu - \zeta e A^\mu - U_0 \delta_0^\mu) - M + U_s - \frac{e\kappa}{4M} \sigma_{\mu\nu} (\partial^\mu A^\nu - \partial^\nu A^\mu) \right] \psi_\alpha(x) = 0, \quad (1)$$

where  $\kappa$  is the anomalous magnetic moment (AMM),  $e$  is the elementary charge and  $\zeta = \pm 1$  is the sign of the particle charge.  $U_s$  and  $U_0$  are the scalar field and time components of the vector field, respectively.

In our model charged particles are protons and electrons. The mean-fields are taken to be zero for electrons, while for protons they are given by relativistic mean-field (RMF) theory [16]. The single

particle energy is then written as

$$E(n, p_z, s) = \sqrt{p_z^2 + (\sqrt{2eBn} + M^{*2} - se\kappa B/2M)^2} + U_0 \quad (2)$$

with  $M^* = M - U_s$ , where  $n$  is the Landau number,  $p_z$  is a  $z$ -component of momentum, and  $s = \pm 1$  is the spin. The vector-field  $U_0$  plays the role of shifting the single particle energy and does not contribute to the result of the calculation. Hence, we can omit the vector field in what follows.

The weak interaction part of the Lagrangian density is written as

$$\mathcal{L}_W = G_F \bar{\psi}_\nu \gamma_\mu (1 - \gamma_5) \psi_\nu \sum_\alpha \bar{\psi}_\alpha \gamma_\mu (c_V - c_A \gamma_5) \psi_\alpha, \quad (3)$$

where  $\psi_\nu$  is the neutrino field,  $\psi_\alpha$  is the field of the particle  $\alpha$ , where  $\alpha$  indicates the proton or electron, while  $G_F$ ,  $c_V$  and  $c_A$  are the coupling constants for the weak interaction [15].

By using the above wave function and interaction, we obtain the differential decay width of the protons and electrons into  $\nu\bar{\nu}$ -pairs.

$$d\Gamma(n_i, n_f) = \frac{G_F^2}{2^9 \pi^5} \frac{N_{\mu\nu} L^{\mu\nu}}{|\mathbf{k}_i| |\mathbf{k}_f| E_i E_f} \delta(P_{iz} - P_{fz} - k_{iz} - k_{fz}) \delta(E_i - E_f - |\mathbf{k}_i| - |\mathbf{k}_f|) d\mathbf{k}_i d\mathbf{k}_f dP_{fz}.$$

with

$$L_{\mu\nu} = 2(k_{f\mu} k_{i\nu} + k_{i\mu} k_{f\nu} - g_{\mu\nu} (k_f \cdot k_i) + i\varepsilon_{\mu\nu\alpha\beta} k_f^\alpha k_i^\beta), \quad (4)$$

$$N_{\mu\nu} = \frac{1}{4} \text{Tr} \int dx_1 dx_2 \tilde{F}_f(x_1 - Q_T/2) \rho_M(n_f, s_f, P_{fz}) \tilde{F}_f(x_2 + Q_T/2) \gamma_\mu (c_V - c_A \gamma_5) \\ \times \tilde{F}_i(x_2 - Q_T/2) \rho_M(n_i, s_i, P_{iz}) \tilde{F}_i(x_1 + Q_T/2) \gamma_\nu (c_V - c_A \gamma_5), \quad (5)$$

where

$$\rho_M(n, s, P_z) = \left[ E\gamma_0 + \sqrt{2eBn}\gamma^2 - p_z\gamma^3 + M^* + (e\kappa B/2M)\Sigma_z \right] \\ \times \left[ 1 + \frac{s}{\sqrt{2eBn} + M^{*2}} (e\kappa B/2M + p_z\gamma_5\gamma_0 - E\gamma_5\gamma^3) \right], \quad (6)$$

and

$$\tilde{F} = \text{diag}(h_n, h_{n-1}, h_n, h_{n-1}) = h_n \frac{1 + \Sigma_z}{2} + h_{n-1} \frac{1 - \Sigma_z}{2} \quad (\text{proton}), \quad (7)$$

$$\tilde{F} = \text{diag}(h_{n-1}, h_n, h_{n-1}, h_n) = h_{n-1} \frac{1 + \Sigma_z}{2} + h_n \frac{1 - \Sigma_z}{2} \quad (\text{electron}). \quad (8)$$

Here,  $\gamma^2$  and  $\gamma^3$  denote the second and third Dirac gamma matrices, respectively,  $\Sigma_z \equiv \text{diag}(1, -1, 1, -1)$ , and  $h_n(x)$  is the harmonic wave function with the quantum number  $n$ .

In actual calculations, we use the parameter-sets of Ref. [17] for the equation of state (EOS) of neutron-star matter, which we take to be comprised of neutrons, protons and electrons. In this work we take the temperature to be very low,  $T \ll 1$  MeV, and use the mean-fields obtained at zero temperature.

In Fig. 1, we show the temperature dependence of the neutrino luminosity per nucleon at  $B = 10^{15}$  G for baryon densities of  $\rho_B = 0.1\rho_0$  (a),  $\rho_B = 0.5\rho_0$  (b) and  $\rho_B = \rho_0$  (c), where  $\rho_0$  is the normal nuclear matter density. The solid, dot-dashed and dashed lines represent the contributions from protons with the AMM, without the AMM, and electrons, respectively. For comparison, we show the neutrino luminosities from the modified Urca (MU) process [18] with the dotted lines.

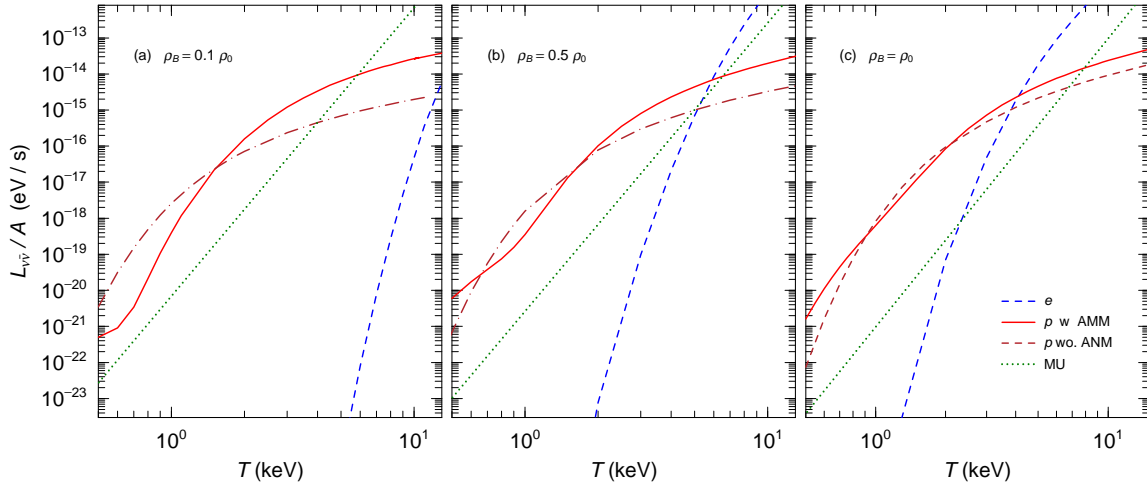


Figure 1:  $\nu\bar{\nu}$ -pair emission luminosity per nucleon versus temperature at the baryon densities  $\rho_B = 0.1\rho_0$  (a),  $\rho_B = 0.5\rho_0$  (b) and  $\rho_B = \rho_0$  (c) for  $B = 10^{15}$  G. The dashed line shows the contribution from electron, and the solid and dot-dashed lines represent those from proton with and without the AMM, respectively. The dotted lines indicate the results with the modified Urca process.

First, we note that in the moderate temperature region,  $T \gtrsim 3-5$  keV, the luminosities change rapidly while they vary slowly in the higher temperature region. This qualitative behavior is very similar to the axion luminosities in Ref. [14].

The energy of the  $\nu\bar{\nu}$ -pair for a charged particle transition is obtained as

$$\begin{aligned}
e_\nu + e_{\bar{\nu}} &= E(n_i, p_z, s_i) - E(n_f, p_z - q_z, s_f) \\
&= \sqrt{2eBn_i + p_z^2 + M^{*2}} - \sqrt{2eB(n_i - \Delta n_{if}) + (p_z - q_z)^2 + M^{*2}} - \frac{e\kappa B}{M} \Delta s_{if} \\
&\approx \frac{eB}{\sqrt{2eBn_i + p_z^2 + M^{*2}}} \Delta n_{if} + \frac{p_z q_z}{\sqrt{2eBn_i + p_z^2 + M^{*2}}} - \frac{e\kappa B}{M} \Delta s_{if},
\end{aligned} \tag{9}$$

where  $\Delta n_{if} = n_i - n_f$ ,  $\Delta s_{if} = (s_i - s_f)/2$ , and  $n_{i,f} \gg E/\sqrt{eB}$  is assumed.

The initial and final states are near the Fermi surface in the low temperature region, and  $|q_z| \ll \sqrt{eB}$ , so that the energy interval of the dominant transition is given by

$$e_\nu + e_{\bar{\nu}} \approx \Delta E = \frac{eB}{E_F^*} \Delta n_{if} - \frac{e\kappa B}{M} \Delta s_{if}. \quad (10)$$

with  $E_F^* = E_F - U_0$ , where  $E_F$  is the Fermi energy.

The luminosities are proportional to the Fermi distribution of the initial state and the Pauli-blocking factor of the final state,  $f(E_i)[1 - f(E_f)]$ . When  $T \ll E_F^*$ , the strength is concentrated in the narrow energy region between  $E_F^* - T$  and  $E_F^* + T$  for both the  $E_i$  and the  $E_f$ . When  $T \lesssim \Delta E \approx eB/E_F^*$ , however, neither the initial nor the final states reside in the region,  $E_F^* - T \lesssim E_{i,f} \lesssim E_F^* + T$ . Then, the luminosities rapidly decrease at low temperature as the temperature becomes smaller as can be seen in Fig. 1. For example, when  $B = 10^{15}$  G, we find that  $eB/E_F^* = 9.4$  keV at  $\rho_B = \rho_0$  for protons. Indeed, the change of the  $\nu\bar{\nu}$ -pair luminosities becomes more abrupt for  $T \lesssim eB/E_F^*$ .

The energy step is much larger for protons than electrons because the proton mass is much larger than the electron mass, and the emission from protons becomes the dominant source of  $\nu\bar{\nu}$ -pairs.

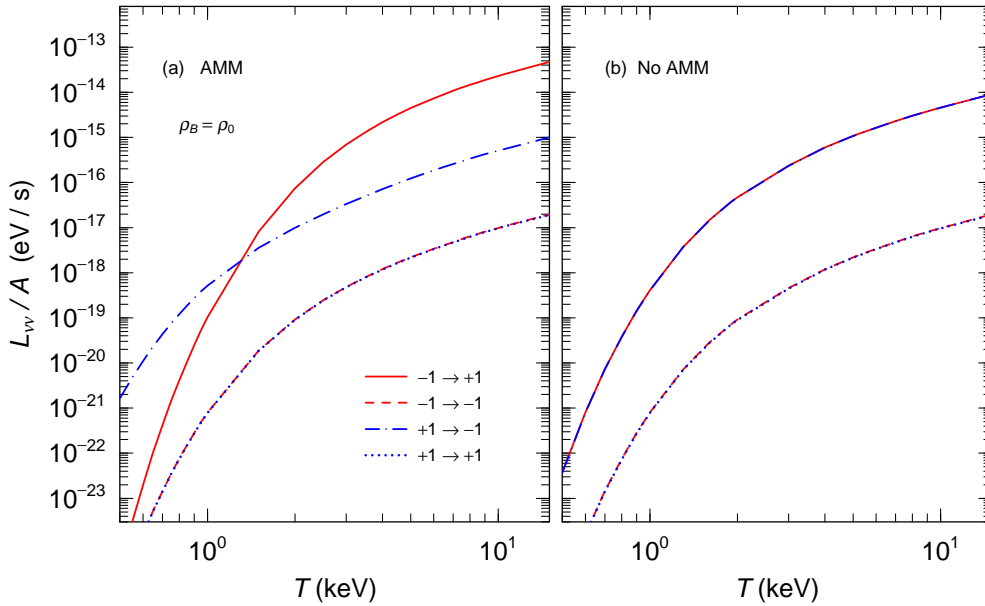


Figure 2: Proton contribution to the  $\nu\bar{\nu}$ -pair emission luminosity per nucleon versus temperature at a baryon density of  $\rho_B = \rho_0$  for  $B = 10^{15}$  G. The left and right panels exhibit the results when the AMM is included and not included, respectively. The solid, dotted, dot-dashed and dotted lines represent the contributions when  $s_i = -s_f = -1$ ,  $s_i = s_f = -1$ ,  $s_i = -s_f = +1$  and  $s_i = s_f = +1$ , respectively. For the result displayed in the left panel, there are no discernable differences between the dotted and dashed lines. This shows that the AMM does not affect the results in the spin non-flip transition. Similarly, in the right panel there are no differences between the dotted and dashed lines and between the solid and dot-dashed lines in the right panel.

In Fig. 2, we show the initial and final spin dependence of  $\nu\bar{\nu}$ -pair luminosities for protons at  $B = 10^{15}\text{G}$  and  $\rho_B = \rho_0$ , when the proton AMM is included (a) and not included (b).

Without the AMM ( $\kappa_p = 0$ ) (b), the contributions from the spin-flip transition,  $s_i = -s_f$ , are about 500 to 1000 times larger than those of the spin non-flip,  $s_i = s_f$ .

With the AMM (a), the transitions of  $s_i = -1 = -s_f$  is dominant in the higher temperature region while the transition  $s_i = +1 = -s_f$  becomes dominant in the lower temperature region. When  $\rho_B = \rho_0$  and  $B = 10^{15}\text{G}$ , we find that  $eB/E_F^* = 9.4\text{ keV}$  and  $e\kappa B/M = 11.30\text{ keV}$ . Thus,  $eB/E_F^* < e\kappa B/M$ , and the transition with  $\Delta n_{if} = n_i - n_f = 2$  gives a dominant contribution for  $s_i = -1 = -s_f$  while the other transition gives the largest contribution. For  $\Delta n_{if} = 1$  the  $\nu\bar{\nu}$ -pair production energy in Eq. (10) is given by  $\Delta E \approx 21\text{ keV}$  when  $s_i = -1 = -s_f$  and  $\Delta E \approx 7.5\text{ keV}$  when  $s_i = +1 = -s_f$ . When the temperature is high enough, this positive additional energy  $e\kappa B/M$  causes the luminosity to increase. This sort of behavior has also been seen in the pion production [12]. When the temperature is very low, however, the positive additional energy makes the energy interval  $\Delta E$  larger than the temperature, and it suppresses the luminosity. The roles of the two contributions reverse at temperatures above the inflections in Fig. 1.

In Fig. 3, we show the density dependence of the luminosities at a temperature of  $T = 0.5, 0.7$  and  $1\text{ keV}$ . The solid and dashed lines represent the contributions from the protons and electrons, respectively. For comparison, we give the  $\bar{\nu}$ -luminosities from the modified Urca (MU) process. In addition, we plot the proton contribution without the AMM and the axion luminosity [14] at  $T = 0.7\text{ keV}$  on the right panel (b), where the strength of the luminosity is taken to be  $10^{-2}$  of that in Ref. [14].

The calculation results include fluctuations. The density dependence of the factor  $f(E_i)[1 - f(E_f)]$  does not smoothly vary for strong magnetic fields and very low temperatures because the energy intervals between the initial and final states are larger than the temperature as discussed above. However, these fluctuations are much smaller than that of the axion luminosity because the invariant mass of the  $\nu\bar{\nu}$ -pair is not fixed while the axion mass is approximately zero.

The proton contributions are dominant at least when  $\rho_B < 3\rho_0$ . The energy intervals for electrons are much larger than those for protons because the electron mass is much smaller than the proton mass. When the AMM does not exist, the electron contributions rapidly increase while the proton contribution gradually decreases.

At  $\rho_B = 0$  and  $B = 10^{15}\text{ G}$ ,  $eB/m_e \approx 11.6\text{ MeV}$  for electrons, and  $eB/M \approx 6.3\text{ keV}$  for protons. For electrons the energy interval is too large, and the transition probability is negligibly small around zero density, while the energy interval for protons is also large but much smaller than that for electrons, and the proton contribution gives a finite value.

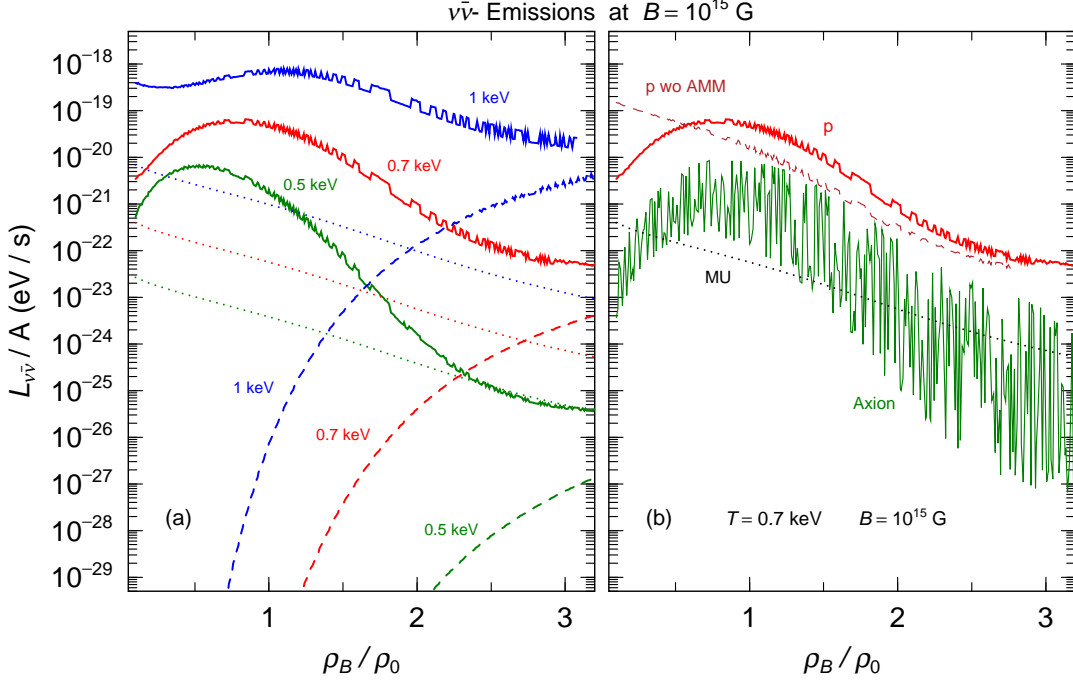


Figure 3: Left panel: Density dependence of the  $\nu\bar{\nu}$ -pair emission luminosity per nucleon for  $B = 10^{15}$  G at  $T = 0.5, 0.7$  and  $1$  keV (from bottom to top). The solid and dashed lines represent the contributions from protons and electrons. The dotted lines indicate the neutrino luminosities from the MU process. Right panel: Luminosity per nucleon for  $B = 10^{15}$  G at  $T = 0.7$  keV. The solid and dashed lines represent the  $\nu\bar{\nu}$ -pair emission luminosity from protons with and without the AMM, respectively. The thin line indicates the axion luminosity.

As the density becomes larger, the Fermi energy of the electrons rapidly increases in the low density region, and the electron contribution increases. In contrast, the effective Fermi energy  $E_F^*$  for protons gradually decreases with increasing the density because of the density dependence of the effective mass  $M^*$ , and that fact that the contribution from protons without the AMM gradually decreases. We should note that  $E_F^*$  increases in the higher density region, and that the proton contributions to the  $\nu\bar{\nu}$ -luminosities must increase at higher densities.

When the AMM is included, we see that there are peaks in the proton contribution around  $\rho_B \approx 0.5 - 1.2\rho_0$ . At  $\rho_B \approx 0.7\rho_0$ ,  $eB/E_F^* \approx e\kappa B/M$ , so that in the low density region, where  $e\kappa B/M \geq eB/E_F^*$ ,  $\Delta n_{If} \geq 2$  for the transition of  $s_I = -s_f = -1$ , and  $\Delta n_{If} \leq -1$  for that of  $s_I = -s_f = -1$ . The density dependence of the transition ratio is different between the two density regions; this change becomes more clear as the temperature decreases. Indeed, when the AMM becomes larger, the difference is critical, and the neutrino luminosity shows different peaks in the two density regions.

In Fig. 4 we show the density dependence of the  $\nu\bar{\nu}$ -luminosities at  $B = 5 \times 10^{14}$  G,  $B = 10^{15}$  G

and  $B = 2 \times 10^{15}$  G. We see that as the magnetic field strength increases, the luminosity decreases in the density region,  $\rho_B/\rho_0 \gtrsim 1$ .

As the magnetic field strength increases, the momentum transfer from the magnetic field becomes larger, and the energy interval between the initial and final states is also larger. The former effect enhances the emission rate, but the latter effect suppresses it. In the region of the magnetic field for magnetars, the latter effect is larger. Indeed, the axion production is largest around  $B = 10^{14}$  G [14].

Thus, the  $\nu\bar{\nu}$ -pair emission process has a much larger effect than that of the MU process in strong magnetic fields. We can conclude that the  $\nu\bar{\nu}$ -pair emission process is dominant in the low density region,  $\rho_B \lesssim \rho_0$ , for a cooling process of magnetars whose magnetic field strength is  $10^{14} - 10^{15}$  G. In the high density region,  $\rho_B \gtrsim 3\rho_0$ , the direct Urca process must appear, and its contribution is much larger than that of the  $\nu\bar{\nu}$ -pair emission.

In summary, we have studied the  $\nu\bar{\nu}$ -pair emission from neutron-star matter with a strong magnetic field,  $B \approx 10^{15}$  G, in a relativistic quantum approach. We calculated the  $\nu\bar{\nu}$ -pair luminosities due to the transitions of protons and electrons between different Landau levels. In such strong magnetic fields the quantum calculation is necessary because the energies of  $\nu\bar{\nu}$ -pairs are much larger than the temperature. In the semi-classical calculations energies of the  $\nu\bar{\nu}$ -pairs are assumed to be almost zero, and the momentum transfer from the magnetic field cannot be taken into account exactly. This would cause the neutrino energy spectra to shift to lower energies in the semi-classical calculation, resulting in a much smaller total luminosity than that of the quantum calculations.

In actual magnetars the magnetic field is weaker than  $10^{15}$  G in the low density region, so that in low density region the  $\nu\bar{\nu}$ -pair luminosity is expected to be much larger than that of neutrinos due to the MU

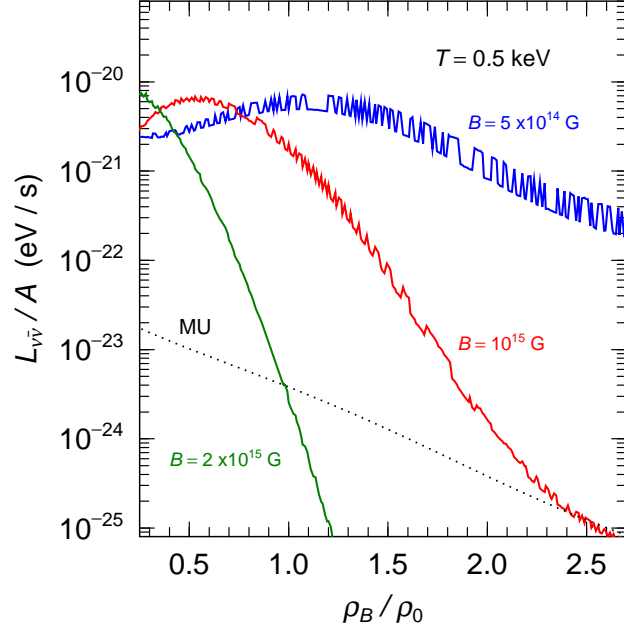


Figure 4: Solid lines show the density dependence of the  $\nu\bar{\nu}$ -pair emission luminosity per nucleon for  $B = 5 \times 10^{14}$  G,  $10^{15}$  G and  $2 \times 10^{15}$  G at  $T = 0.5$  keV. The dotted lines indicate the neutrino luminosity from the MU process.



process. Therefore, the present results suggest that one needs to introduce the  $\nu\bar{\nu}$ -pair emission process when calculating the cooling rate of magnetars.

We expect that the cooling rate would increase due to the  $\nu\bar{\nu}$ -pair emission process. On the other hand, additional energy made by transitions between Landau levels could contribute to high energy part of the thermal spectra of neutrinos and anti-neutrinos, which may heat the ambient gas surrounding magnetars through absorption. Thus, the  $\nu\bar{\nu}$ -pair production process may contribute to both the heating and cooling of magnetars whose surface temperature is larger than that of normal neutron stars. More careful calculations of neutrino transport including these processes are highly desirable to quantify this speculation.

This work was supported in part by the Grants-in-Aid for the Scientific Research from the Ministry of Education, Science and Culture of Japan (JP19K03833, JP17K05459, JP16K05360, JP15H03665). ABB is supported in part by the U.S. National Science Foundation Grant No. PHY-1806368. MKC is supported by the National Research Foundation of Korea (Grant Nos. NRF-2017R1E1A1A01074023, NRF-2013M7A1A1075764). Work of GJM supported in part by the U.S. Department of Energy under Nuclear Theory Grant DE-FG02-95-ER40934.

## References

- [1] B. Paczyński, *Acta. Astron.* **41** (1992) 145.
- [2] For a review, G. Chanmugam, *Annu. Rev. Astron. Astrophys.* **30** (1992) 143.
- [3] S. Mereghetti, *Annu. Rev. Astron. Astrophys.*, **15** (2008) 225.
- [4] A.D. Kaminker et al. *MNRAS* 2009; 395: 2257-2267.
- [5] D.G. Yakolev and C.J. Pethick, *Ann. Rev. Astron. Astrophys.*, **42** (2004) 169.
- [6] J.D. Landstreet. *Phys. Rev.* **153** (1966) 1372.
- [7] A.D. Kaminker, K.V. Levenfish, and D.G. Yakolev, *Phys. Rev.* **D46**, 3256 (1992).
- [8] A. Vidaurre, A. Perez, H. Sivak, J. Bernabeu, J.M. Ibanez, *Ap.J.* **448** (1995) 264.
- [9] E.N.E. van Dalen, A.E.L. Dieperink, A. Sedrakian and R.G.E. Timmermans, *Astron. Astrophys.* 360 (2000) 549

- [10] A.D. Kaminker, C.J. Pethick, A.Y. Potekhin, V. Thorsson, and D.G. Yakovlev, *Astron. Astrophys.* **343** (1999) 1009.
- [11] D.D. Ofengeim<sup>1,2</sup>, A.D. Kaminker and D.G. Yakovlev, *EPL*, **108** (2014) 31002
- [12] T. Maruyama, M.-K. Cheoun, T. Kajino, Y. Kwon, G.J. Mathews, C.Y. Ryu, *Phys. Rev.* **D91** (2015) 123007.
- [13] T. Maruyama, M.-K. Cheoun, T. Kajino, G.J. Mathews, *Phys. Lett.* **B75** (2016) 125.
- [14] T. Maruyama, A.B. Balantekin, M.-K. Cheoun, T. Kajino, G.J. Mathews, *Phys. Lett.* **B** (2018).
- [15] S. Reddy, M. Prakash and J.M. Lattimer, *Phys. Rev.* **D58** (1998) 013009.
- [16] B.D. Serot and J.D. Walecka, *Int. J. Mod. Phys.* **E6**, 515 (1997).
- [17] T. Maruyama, J. Hidaka, T. Kajino, N. Yasutake, T. Kuroda, T. Takiwaki, M.K. Cheoun, C.Y. Ryu, G.J. Mathews, *Phys. Rev.* **D90**, 067302 (2014) .
- [18] O.V. Maxwell, *ApJ* **319**, 691 (1987); D.G. Yakolev, K.P. Levenfish *A&A* **297** (1995) 717.
- [19] L.B. Leinson, *Nucl. Phys.* **A707** (2002) 543.